

The Influence of Relativistic Effects on Nuclear Magnetic Resonance Spin–Spin Coupling Constant Polarizabilities of H_2O_2 , H_2S_2 , H_2Se_2 , and H_2Te_2

Gabriel I. Pagola,¹ Martin A. B. Larsen,² Marta Ferraro¹ and Stephan P. A. Sauer²

Relativistic and nonrelativistic calculations have been performed on hydrogen peroxide, dihydrogen disulfide, dihydrogen diselenide, and dihydrogen ditelluride, H_2X_2 ($\text{X} = \text{O}, \text{S}, \text{Se}, \text{Te}$), to investigate the consequences of relativistic effects on their structures as well as their nuclear magnetic resonance (NMR) spin–spin coupling constants and spin–spin coupling constant polarizabilities. The study has been performed using both one-component nonrelativistic and four-component relativistic calculations at the density functional theory (DFT) level with the B3LYP exchange–correlation functional. The calculation of nuclear spin–spin coupling constant polarizabilities has

been performed by evaluating the components of the third order tensor, nuclear spin–spin coupling polarizability, using quadratic response theory. From this, the pseudoscalar associated with this tensor has also been calculated. The results show that relativistic corrections become very important for H_2Se_2 and H_2Te_2 and hint that a new chiral discrimination technique via NMR spectroscopy might be possible for molecules containing elements like Se or Te. © 2018 Wiley Periodicals, Inc.

DOI:10.1002/jcc.25648

Introduction

Structural characterization of chemical compounds is one of the foundations of chemical research as it serves as a bridgehead to understanding mechanisms and reactivity of chemical species. Nuclear magnetic resonance (NMR) spectroscopy is one of such techniques that have proven powerful and valuable to determine the structures of molecules in solution, gas, and solid phase. However, the chemical shifts and spin–spin coupling constants of NMR do not differentiate between enantiomers—the measured response is identical. So far the available options to recognize mirror structures by NMR have been limited to the addition of chiral solvents or reagents.^[1–4] Buckingham's theoretical work, however, has suggested the possibility of observing chirality in NMR by application of an electric field.^[5,6] The measurements would require an experimental setup a little different from the standard NMR spectrometers but the effect is in principle observable.^[7,8] The properties leading to different measurements in NMR for enantiomers are the nuclear spin–spin coupling constant polarizabilities (and/or the nuclear magnetic shielding polarizabilities) and for the gas or liquid phase, it is possible to define a pseudo-scalar that has equal but opposite values for enantiomers.^[6] Previous calculations have indicated that the effect is very small and a huge electric field would have to be applied to observe a difference with the resolution achievable with present-day NMR spectrometers.^[9–11] Nevertheless, it was early on suggested that the effect would be more pronounced for heavier nuclei.^[5] From this perspective, the previous efforts have been directed at molecules containing rather light nuclei with the heaviest atoms being oxygen. The only exception is a nonrelativistic study of the pseudoscalar of the shielding

polarizability for the cyclic $\text{C}_4\text{H}_2\text{X}_2$ molecules, with $\text{X} = \text{O}, \text{S}, \text{Se},$ and Te .^[12] As the computational cost increases rapidly with heavier nuclei it is necessary to restrict the calculations to small model systems. Therefore, a series of hydrogen peroxide-like molecules have been chosen for this study— H_2O_2 , H_2S_2 , H_2Se_2 , and H_2Te_2 . These molecules are just large enough to be chiral in their equilibrium structure and due to their obvious similarity should allow for a seemingly straightforward comparison of properties. Regarding the level of theory none of the previous investigations has been performed using a fully relativistic treatment of the systems and this work presents the first results doing so, as during the last years there has been a great effort to provide NMR spectroscopic parameters considering relativistic effects at the four-component level.^[13] The treatment of electron correlation is

[a] G. I. Pagola, M. Ferraro

Departamento de Física, Facultad de Ciencias Exactas y Naturales, Universidad de Buenos Aires and IFIBA, CONICET, Ciudad Universitaria, Pabellón 1, (1428) Buenos Aires, Argentina
E-mail: gpagola@df.uba.ar

[b] M. A. B. Larsen, S. P. A. Sauer

Department of Chemistry, University of Copenhagen, Universitetsparken 5, DK-2100, Copenhagen Ø, Denmark

Memory: This article is written in memory of the late Professor Rubén Horacio Contreras (University of Buenos Aires), the then Associate Editorial Board Member of *Magnetic Resonance in Chemistry*, and late Professor Martín Ruiz de Azúa, who made important contributions to the proper description of relativistic effects on Nuclear Magnetic Resonance nuclear shieldings.

Contract Grant sponsor: Consejo Nacional de Investigaciones Científicas y Técnicas; Contract Grant number: PIP 11220130100377; Contract Grant sponsor: Universidad de Buenos Aires; Contract Grant number: UBACYT 20020130100039BA and 20020130200096BA

© 2018 Wiley Periodicals, Inc.

done at the level of density functional theory with the functional B3LYP.

The aim of this article is, thus, to investigate whether the spin-spin coupling constant polarizabilities will increase with increasing nuclear charge in this series of molecules and how large the relativistic contributions to this effect might be. After defining the relevant properties both in the nonrelativistic and in the four-component relativistic domain, we will first discuss the effects of relativity on the geometry of these molecules and study their basis set dependence. Second, we will present the results of nonrelativistic and relativistic calculations of the spin-spin coupling constants in this series of molecules before thirdly discussing the spin-spin coupling constant polarizabilities. In summary, these calculations will clarify when the nuclear charge has become large enough for relativistic effects to play a role at the structural level and whether this limit is equivalent to the limit for the calculation of spin-spin coupling constants.

Theory of Spin-Spin Coupling Constant Polarizabilities

The total energy of a molecule in the presence of intramolecular perturbations, that is, the permanent magnetic dipoles $m_I = \gamma_I \mathbf{I}_I$, and $m_J = \gamma_J \mathbf{I}_J$ expressed via the magnetogyric ratios γ_I and γ_J and spins \mathbf{I}_I and \mathbf{I}_J of two nuclei I and J , and an external time-independent, spatially uniform electric field \mathbf{E} , is

$$W = W^{(0)} + \sum_{J < I} \sum_{\alpha\beta\gamma} m_{I\alpha} K_{I\alpha J\beta} m_{J\beta} + \sum_{J < I} \sum_{\alpha\beta\gamma} m_{I\alpha} K_{I\alpha J\beta}^{\gamma} m_{J\beta} E_{\gamma} + \dots \quad (1)$$

where

$$K_{I\alpha J\beta} = \left. \frac{\partial W}{\partial m_{I\alpha} \partial m_{J\beta}} \right|_{m_I, m_J, E \rightarrow 0} \quad (2)$$

and the polarizability of the reduced nuclear spin-spin coupling is a third-rank tensor obtained as the third derivative of the energy, eq. 1

$$K_{I\alpha J\beta}^{\gamma} = \left. \frac{\partial W}{\partial m_{I\alpha} \partial m_{J\beta} \partial E_{\gamma}} \right|_{m_I, m_J, E \rightarrow 0} \quad (3)$$

The reduced nuclear spin-spin coupling tensor in the presence of an applied electric field can be expanded as a Taylor series:

$$K_{I\alpha J\beta}^{\gamma}(E) = K_{I\alpha J\beta}^{\gamma} + \sum_{\gamma'} K_{I\alpha J\beta}^{\gamma\gamma'} E_{\gamma'} \quad (4)$$

where

$$K_{I\alpha J\beta}^{\gamma} = K_{I\alpha J\beta}^{\gamma}(0) \quad (5)$$

The reduced nuclear spin-spin coupling tensor components are related to those of $J_{I\alpha J\beta}^{\gamma}$ tensor, usually expressed in Hertz by

$$K_{I\alpha J\beta}^{\gamma} = 4\pi^2 \frac{J_{I\alpha J\beta}^{\gamma}}{h\gamma_I \gamma_J} \quad (6)$$

with analogous relationships for the coupling polarizability

$$K_{I\alpha J\beta}^{\gamma} = 4\pi^2 \frac{J_{I\alpha J\beta}^{\gamma}}{h\gamma_I \gamma_J} \quad (7)$$

Three quantities will be considered in the results section, the isotropic reduced coupling

$$K^{IJ} = \frac{1}{3} \sum_{\alpha} K_{I\alpha J\alpha} \quad (8)$$

the electric field derivatives of the isotropic reduced coupling

$$A_{\gamma}^{IJ} = \frac{1}{3} \sum_{\alpha} K_{I\alpha J\alpha}^{\gamma} \quad (9)$$

and a pseudoscalar which vanishes for achiral molecules, that is, an isotropic average:

$$\bar{K}_{IJ}^{(1)} = \frac{1}{6} \sum_{\alpha\beta\gamma} \epsilon_{\alpha\beta\gamma} K_{I\alpha J\beta}^{\gamma} \quad (10)$$

where $\epsilon_{\alpha\beta\gamma}$ is the Levi Civita symbol.^[14]

In nonrelativistic theory the elements of the $K^{I\alpha J\beta}$ coupling tensor are linear response functions^[15,16]

$$K^{I\alpha J\beta} = \left\langle \left\langle \hat{H}_{I\alpha}^{\text{PSO}} + \hat{H}_{I\alpha}^{\text{FC}} + \hat{H}_{I\alpha}^{\text{SD}}; \hat{H}_{J\beta}^{\text{PSO}} + \hat{H}_{J\beta}^{\text{FC}} + \hat{H}_{J\beta}^{\text{SD}} \right\rangle \right\rangle_{\omega=0} + \left\langle 0 \left| \hat{H}_{I\alpha J\beta}^{\text{DSO}} \right| 0 \right\rangle \quad (11)$$

with the exception of the diamagnetic spin-orbit (DSO) operator, which is an expectation value of the ground state $|0\rangle$,^[17] although it can also be reformulated as a linear response function.^[18] The mechanism for Fermi-contact (FC) and spin-dipolar (SD) contributions to coupling constants and their polarizabilities comes from the interaction between the nuclear spin and the spin magnetic moment of the electrons, whereas the interaction between the nuclear spin and the orbital magnetic moments provide a paramagnetic and a diamagnetic spin-orbit contribution, PSO and DSO, respectively.

The $K_{I\alpha J\beta}^{\gamma}$ coupling polarizability tensor components are quadratic response functions,

$$K_{I\alpha J\beta}^{\gamma} = \left\langle \left\langle \hat{H}_{I\alpha}^{\text{PSO}} + \hat{H}_{I\alpha}^{\text{FC}} + \hat{H}_{I\alpha}^{\text{SD}}; \hat{H}_{J\beta}^{\text{PSO}} + \hat{H}_{J\beta}^{\text{FC}} + \hat{H}_{J\beta}^{\text{SD}}; \hat{H}_{\gamma}^{\text{E}} \right\rangle \right\rangle_{\omega, \omega' = 0} + \left\langle \left\langle \hat{H}_{I\alpha J\beta}^{\text{DSO}}; \hat{H}_{\gamma}^{\text{E}} \right\rangle \right\rangle_{\omega=0} \quad (12)$$

with the exception again of the DSO contributions, which are linear response functions, as is outlined in a previous paper.^[9]

The nonrelativistic perturbation operators^[19] are classified in singlet and triplet operators, depending on whether they contain spin or not. Their explicit form is displayed in Table 1, where Θ_S is the spin symmetry (triplet or singlet).

The position vectors of electron i and nucleus K are denoted as \mathbf{r}_i and \mathbf{R}_K , respectively, and $\mathbf{r}_{iK} = \mathbf{r}_i - \mathbf{R}_K$. The electronic angular momentum operator with respect to the position of the nucleus is denoted as $\mathbf{I}_{iK} = (\mathbf{r}_i - \mathbf{R}_K) \times \mathbf{p}_i = \mathbf{r}_{iK} \times \mathbf{p}_i$ and the electronic operator as \mathbf{s}_i . The elementary charge and electronic mass are e and m and g_e is the electronic g-factor.

Table 1. Nonrelativistic perturbation operators and their spin-symmetry Θ_S .		
Perturbation	Operator	Θ_S
E	$\hat{H}_\alpha^E = \sum_i -\mu_{i,\alpha} = \sum_i e r_{i,\alpha}$	S
mκ	$\hat{H}_{K_\alpha}^{\text{PSO}} = \sum_i \hat{h}_{K_\alpha,i}^{\text{PSO}} = \left(\frac{\mu_0}{4\pi}\right) \left(\frac{e}{m}\right) \sum_i \frac{1_{K_\alpha}}{r_{iK}^3}$	S
mκ	$\hat{H}_{K_\alpha}^{\text{SD}} = \sum_i \hat{h}_{K_\alpha,i}^{\text{SD}} = -\left(\frac{\mu_0}{4\pi}\right) \left(\frac{g_e e}{2m}\right) \sum_i \frac{S_{i\alpha} r_{iK}^2 - 3(\mathbf{s}_i \cdot \mathbf{r}_{iK}) r_{iK\alpha}}{r_{iK}^5}$	T
mκ	$\hat{H}_{K_\alpha}^{\text{FC}} = \sum_i \hat{h}_{K_\alpha,i}^{\text{FC}} = \left(\frac{\mu_0}{4\pi}\right) \left(\frac{4\pi g_e e}{3m}\right) \sum_i \delta(\mathbf{r}_{iK}) S_{i\alpha}$	T
mκ mL	$\hat{H}_{K_\alpha L_\beta}^{\text{DSO}} = \sum_i \hat{h}_{K_\alpha L_\beta,i}^{\text{DSO}} = \left(\frac{\mu_0}{4\pi}\right)^2 \left(\frac{e^2}{m}\right) \sum_i \frac{\delta_{\alpha\beta}(\mathbf{r}_{iK} \cdot \mathbf{r}_{iL}) - r_{iL\alpha} r_{iK\beta}}{r_{iK}^3 r_{iL}^3}$	S

In the four-component case, the elements of the $K^{l\alpha j\beta}$ coupling tensor are just one linear response function^[20,21]

$$K^{l\alpha j\beta} = \langle\langle \hat{H}_{l\alpha}; \hat{H}_{j\beta} \rangle\rangle_{\omega=0} \quad (13)$$

as the relativistic analog to the nonrelativistic diamagnetic contribution is included via excitations from occupied positive-energy orbitals to virtual negative-energy orbitals, although an explicit diamagnetic contribution could have been obtained via the Sternheimer approximation.^[22] Correspondingly to eq. 13 also the components of the $K_\gamma^{l\alpha j\beta}$ coupling Polarizability tensor are just one quadratic response function^[23,24]

$$K_\gamma^{l\alpha j\beta} = \langle\langle \hat{H}_{l\alpha}; \hat{H}_{j\beta}; \hat{H}_\gamma^E \rangle\rangle_{\omega, \omega' = 0} \quad (14)$$

The four-component relativistic perturbation operators are given in Table 2. In the relativistic domain the spin-orbit interaction couples spin and spatial degrees of freedom, so the spin symmetry is lost and replaced by time-reversal symmetry, $\Theta_t = \pm 1$, (+ for symmetric and – for anti-symmetric operators), which is also specified in the table.

The Dirac matrices, α , are $\alpha = \begin{bmatrix} \mathbf{O}_2 & \boldsymbol{\sigma} \\ \boldsymbol{\sigma} & \mathbf{O}_2 \end{bmatrix}$ with the Pauli spin matrices $\sigma_x = \begin{bmatrix} 0 & 1 \\ 1 & 0 \end{bmatrix}$, $\sigma_y = \begin{bmatrix} 0 & -i \\ i & 0 \end{bmatrix}$ and $\sigma_z = \begin{bmatrix} 1 & 0 \\ 0 & -1 \end{bmatrix}$.

The methods used to develop the general theory of molecular properties have essentially the same structure in the relativistic and nonrelativistic domain. The theory and implementation of nonrelativistic linear and quadratic response functions at time dependent Hartree–Fock and time dependent density functional theory (DFT) level has been described many times.^[25–29] In the four component regime, the relativistic Hartree–Fock equations were e.g. implemented by Saue et al.^[30] One has to take into account that for the relativistic

Table 2. Relativistic perturbation operators and their time reversal symmetry Θ_t .		
Perturbation	Operator	Θ_t
E	$\hat{H}_\alpha^E = \sum_i -\mu_{i,\alpha} = \sum_i e r_{i,\alpha}$	+1
mκ	$\hat{H}_{K_\alpha} = \sum_i \hat{h}_{K_\alpha,i} = ce \left(\frac{\mu_0}{4\pi}\right) \sum_i \frac{(\boldsymbol{\alpha} \times \mathbf{r}_{iK})_\alpha}{r_{iK}^3}$	-1

case, the orbitals and in consequence the integrals are complex. Also reductions due to symmetry are different, as it is pointed out in many Refs.^[21,31] Linear response functions for external perturbations, in the form of electric or magnetic fields, at the Hartree–Fock or DFT level have been derived by Saue and Jensen.^[21] The derivation will not be repeated here but the final equations are complex and the hermiticity and time reversal symmetry of the operators was considered in the derivation employing a quaternion formulation.^[32] The generic forms of the linear response functions parallels otherwise those found in the nonrelativistic case. The reference state is a single determinant where the one electron functions are complex four-component spinors. Norman and coworkers developed^[23,24] the quadratic response function in the time dependent four-component Hartree–Fock and DFT approximation. They employed again the quaternion symmetry scheme that provides maximum computational efficiency with consideration made to time-reversal and spatial symmetries. In general, the equations for linear and quadratic response are simpler in the relativistic formalism than in the nonrelativistic one, but the generation of four-component wave function is computationally considerably heavier than in the nonrelativistic calculations.

Computational Details

There are three types of calculations for each molecule; structural optimizations, calculation of nuclear spin–spin coupling constants, and the calculation of the spin–spin coupling constant polarizabilities. All relativistic four-component Dirac–Coulomb calculations have been performed using the DIRAC 14.0 or DIRAC 15.0 programs.^[33] The nonrelativistic geometry optimizations have also been run with DIRAC programs while the nonrelativistic calculation of the coupling constants and coupling constant polarizability have been carried out with the Dalton program^[34] as described previously.^[9]

The structural optimizations of hydrogen peroxide have been performed using a guess structure with parameters similar to experimentally determined bond lengths, bond angles, and dihedral angle. The same is true for dihydrogen disulfide while an optimized geometry from dihydrogen disulfide is used as a starting guess for dihydrogen diselenide and dihydrogen ditelluride. The reduced spin–spin coupling constants have been calculated as linear response functions, eq. 13, and only the isotropic reduced coupling constants K^J , eq. 8, are reported. The elements of the reduced coupling constant polarizability tensor have been calculated as quadratic response functions, eq. 14 and both the components of the electric field derivatives of the isotropic reduced coupling constants or reduced coupling constant polarizability vector, A_γ^J , eq. 9, and the pseudoscalar $\bar{K}_J^{(1)}$, eq. 10, are reported in the following.

The underlying theory of DFT does not offer the advantage of knowing which exchange–correlation functionals will perform better than others and so a functional that has previously performed reasonably is often chosen. In the current work, all calculations have been performed with the hybrid exchange–correlation functional B3LYP, as it was shown in previous work

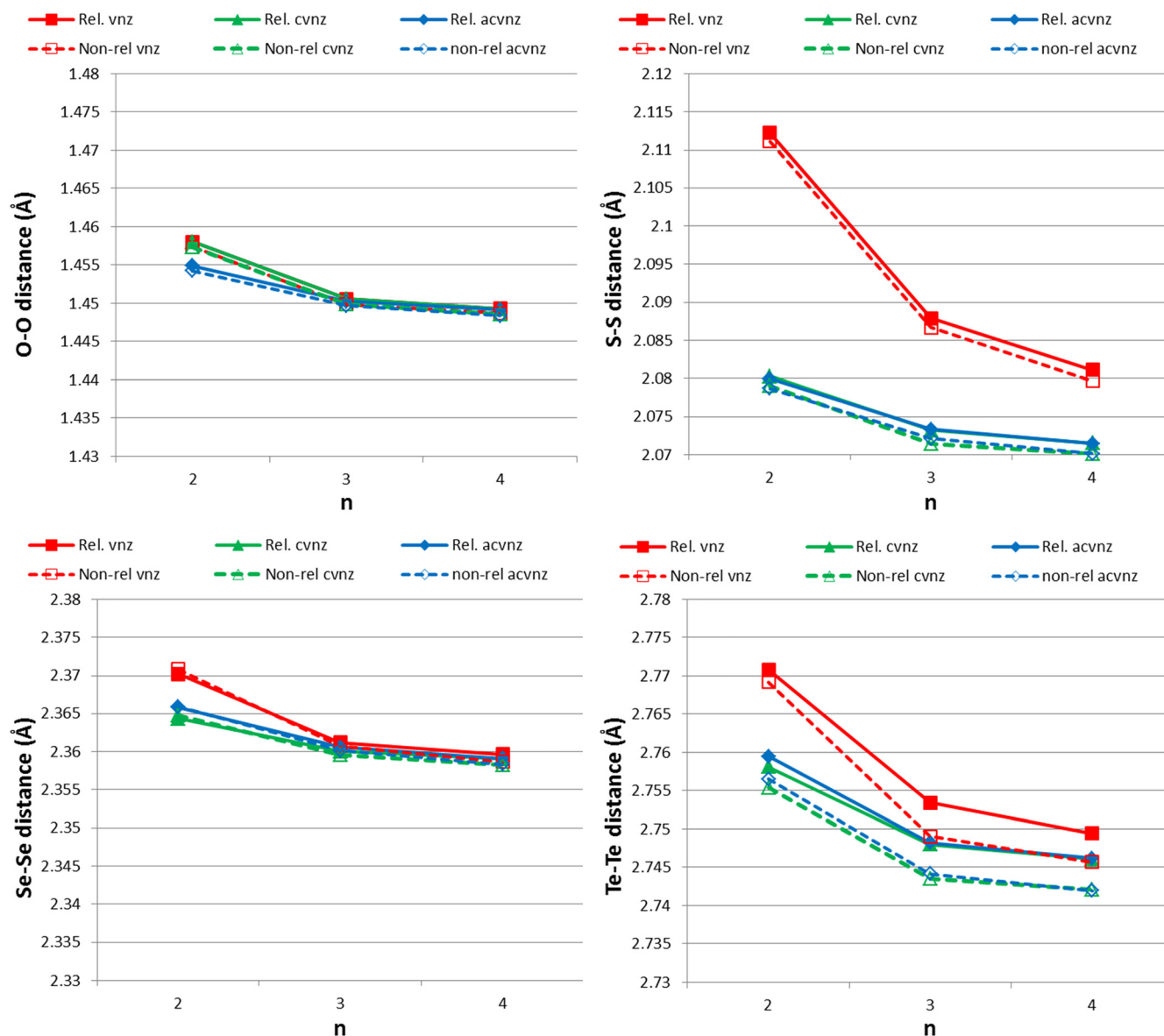


Figure 1. The X-X bond length in Å (X = O, S, Se, Te) versus cardinal numbers n of the dyall.vnz, dyall.cvnz, and dyall.acvnz obtained in four-component ("Rel" and solid lines) and nonrelativistic ("Non-rel" and dashed lines) geometry optimizations using the B3LYP functional. Tables with the values are presented in the Supporting Information. [Color figure can be viewed at wileyonlinelibrary.com]

that there is no general preference for B97-2 or B3LYP when calculating coupling constant polarizabilities.^[10,11]

The basis sets employed in the current work all belong to the families of relativistic basis sets generated by Dyall.^[35] For the structural optimizations the standard series dyall.vnz, the core-valence series dyall.cvnz, and the augmented core-valence series dyall.acvnz all with $n = 2, 3, 4$ were employed. For the subsequent calculation of coupling constants and coupling constant polarizabilities only the largest series dyall.acvnz was employed. These basis sets are not especially optimized for the calculation of spin-spin coupling constants like, for example, the aug-cc-pVTZ-J^[36] or (aug)-pcJ-n basis sets.^[37] However, these core-property basis sets do not exist for all the atoms in our molecules and in addition the previous study on H₂O₂ showed that diffuse functions are important for the coupling polarizabilities.^[11] Conversely, the

uncontracted dyall.av3z basis set had previously been shown to be converged with respect to calculations of one-bond couplings involving tellurium^[38] and certainly for geometries.^[39] All calculations have been performed with uncontracted basis sets as this is a requirement to fulfill the kinetic balance condition of the relativistic calculations. This condition has been retained for the nonrelativistic calculations in the interest of keeping the calculations easily comparable.

Results and Discussion

Basis set dependence and relativistic effects on the geometries

In Figure 1, the basis set dependence of the optimized bond lengths between the non-hydrogen atoms is shown for both

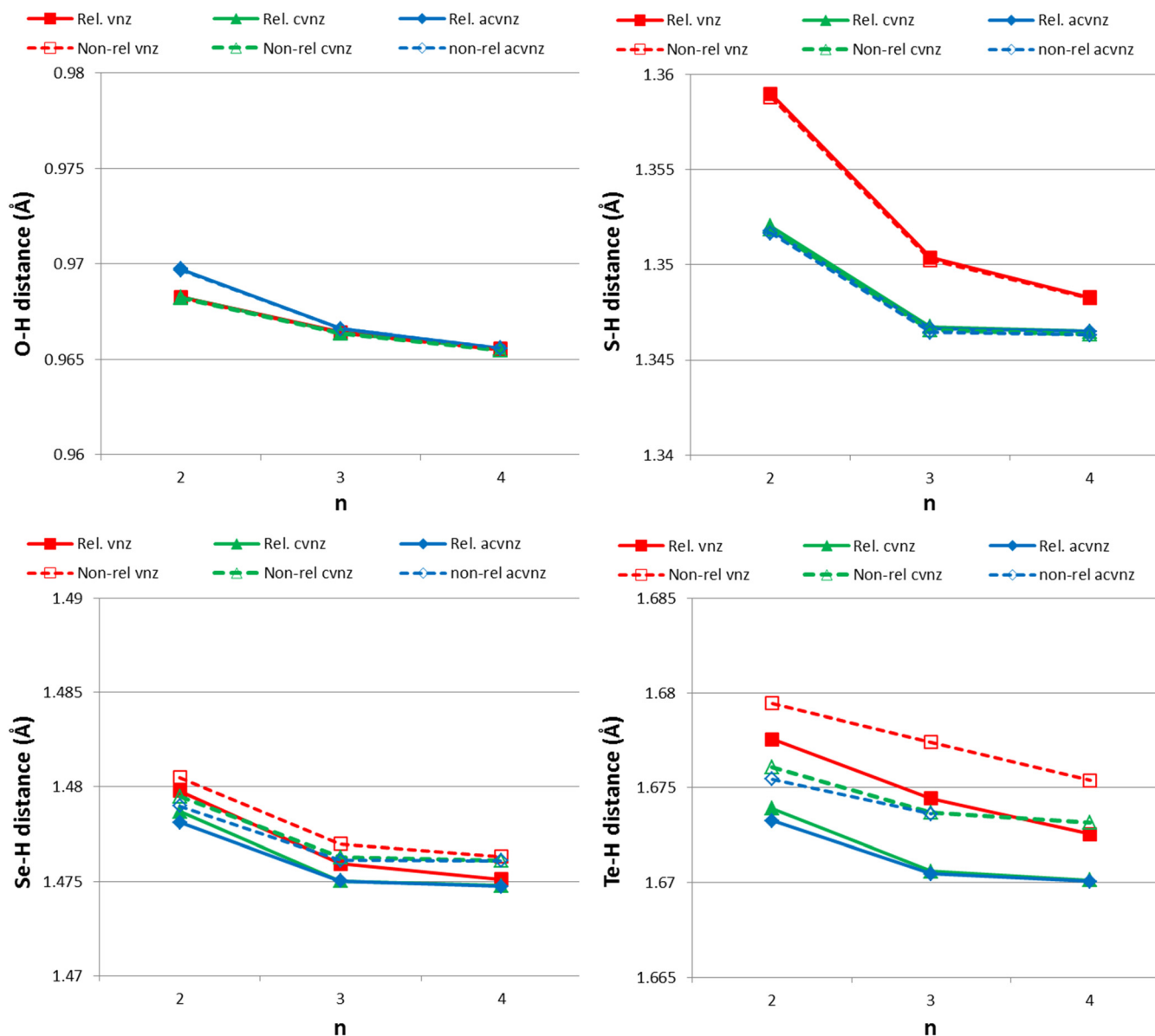


Figure 2. The X-H bond length in Å ($X = O, S, Se, Te$) versus cardinal numbers n of the dyall.vnz, dyall.cvnz, and dyall.acvnz obtained in four-component (“Rel” and solid lines) and nonrelativistic (“Non-rel” and dashed lines) geometry optimizations using the B3LYP functional. Tables with the values are presented in the Supporting Information. [Color figure can be viewed at wileyonlinelibrary.com]

the four-component (solid lines) and nonrelativistic calculations. The first observation is the large difference between the behavior of the dyall.vnz basis sets for O and Se, on one hand, and S and Te on the other. While for the former the bond lengths converge for this series more or less to the same result as with the core-valence basis sets, for S the dyall.v4z bond length deviates by ~ 0.01 Å from the converged value and for Te by about half of this. This points to a deficiency in the set of more compact functions in the dyall.vnz basis sets for S and Te similar to what previously had been observed for cc-pVXZ basis sets of the second third row atoms.^[40] By chance or more precisely by error cancelation the nonrelativistic dyall.v4z Te-Te bond length is actually very close to the converged four-component value. A second observation is that the additional diffuse functions in the dyall.acvnz basis set are not necessary at all. Finally, there is

a clear convergence toward shorter bond lengths with increasing cardinal number n of the basis set for all molecules, as the differences between the $n = 3$ and $n = 4$ basis sets are much smaller than between the $n = 2$ and $n = 3$ basis sets. Sufficiently converged results can, therefore, be obtained already with the dyall.cv3z basis set.

Inclusion of relativistic effects increases the X-X bond length in all molecules. However, the effects are very small. Only in the case of tellurium, the increase amounts to 0.15% which is, thus, larger than the change on going from the triple to the quadruple ζ basis sets. Obviously, there is no relevant relativistic change in the O-O bond length, but it is a bit unexpected to see that the relativistic change in the bond length is smaller for selenium than for sulfur. This might be explained by the fact, that the X-X bonds are mostly formed by p-orbitals, whose

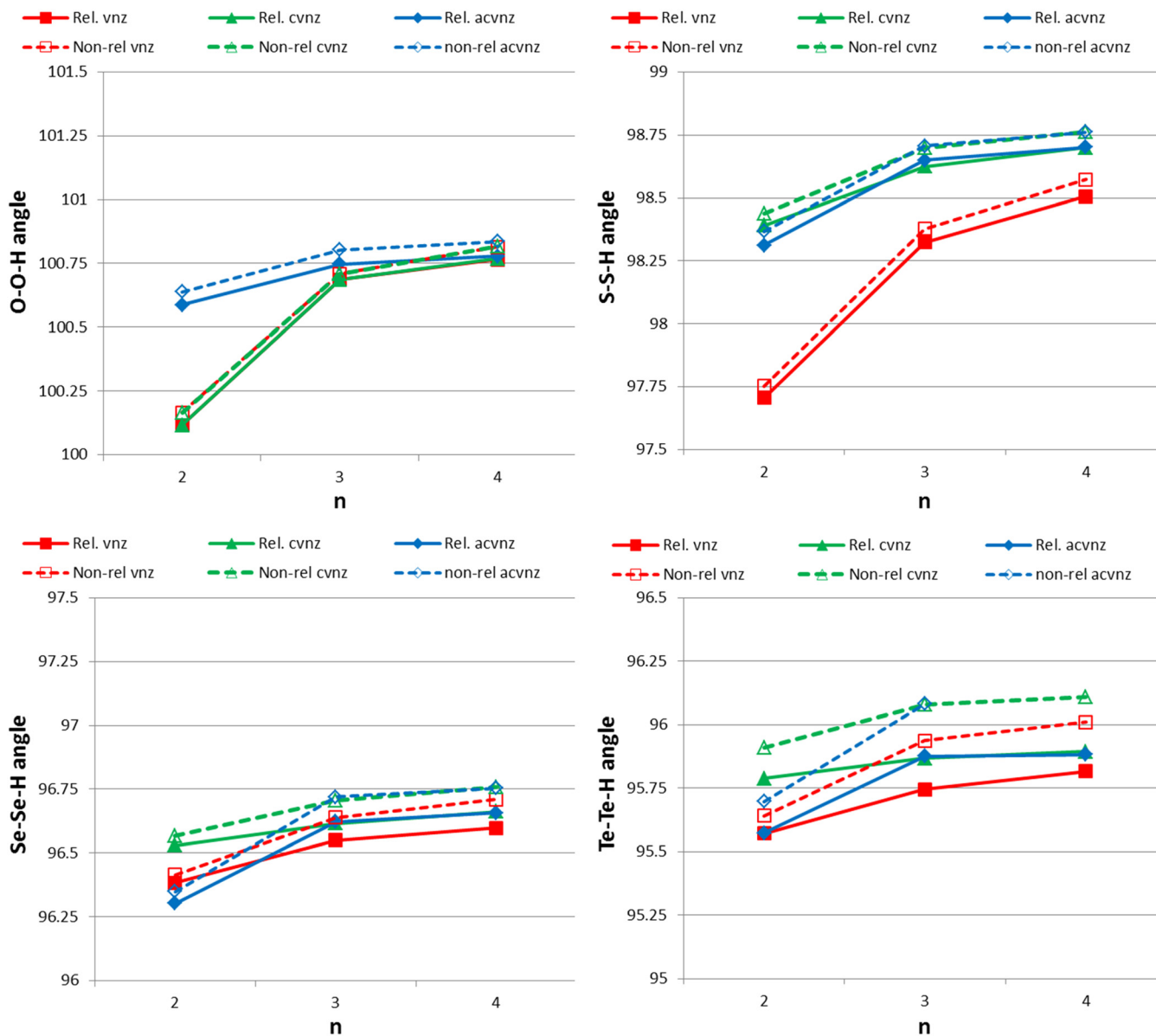


Figure 3. The X-X-H angle ($X = O, S, Se, Te$) versus cardinal numbers n of the dyall.vnz, dyall.cvnz, and dyall.acvnz obtained in four-component ("Rel" and solid lines) and nonrelativistic ("Non-rel" and dashed lines) geometry optimizations using the B3LYP functional. Tables with the values are presented in the Supporting Information. [Color figure can be viewed at wileyonlinelibrary.com]

extent are not as much changed by relativistic effects as, for example, s -orbitals.^[41] On the other hand, it has also been discussed that the relativistic change in the bond lengths is not caused by the change in the extent of the orbitals but by the relaxation of the kinetic repulsion.^[42]

Compared with the experimentally measured bond lengths, $R(O-O) = 1.475 \text{ \AA}$ ^[43] and $R(S-S) = 2.0564 \text{ \AA}$,^[44] our values calculated at the four-component level with the dyall.acv4z basis set, 1.4491 \AA and 2.0715 \AA , differ by 1–2%. While our predicted O-O distance is too short, the S-S distance is slightly too large. Furthermore the deviation in the S-S bond is both percentage-wise and in absolute values smaller than for the O-O bond. For H_2Se_2 and H_2Te_2 our optimized X-X bond lengths are 2.3591 \AA and 2.7462 \AA , respectively, with the dyall.acv4z basis set.

Turning now to the X-H bond lengths in Figure 2 we observe again the large difference between the performance of the dyall.vnz basis sets between O and Se on one side and S and Te on the other. And again there is no need at all for the extra diffuse functions in the dyall.vnz basis sets. Furthermore the triple- ζ results are as good as converged maybe with the slight exception of the O-H bond length in H_2O_2 . Contrary to the X-X bonds, relativistic effects reduce the X-H bond lengths for all the molecules. However, only for Se and Te they are worth mentioning, where they amount to $\sim 0.1\%$ and $\sim 0.2\%$.

Compared with the experimentally measured bond lengths, $R(O-H) = 0.950 \text{ \AA}$ ^[41] and $R(S-H) = 1.3421 \text{ \AA}$,^[42] our values calculated at the four-component level with the dyall.acv4z basis set, 0.9656 \AA and 1.3465 \AA , are now both 2% or 0.3% too long in

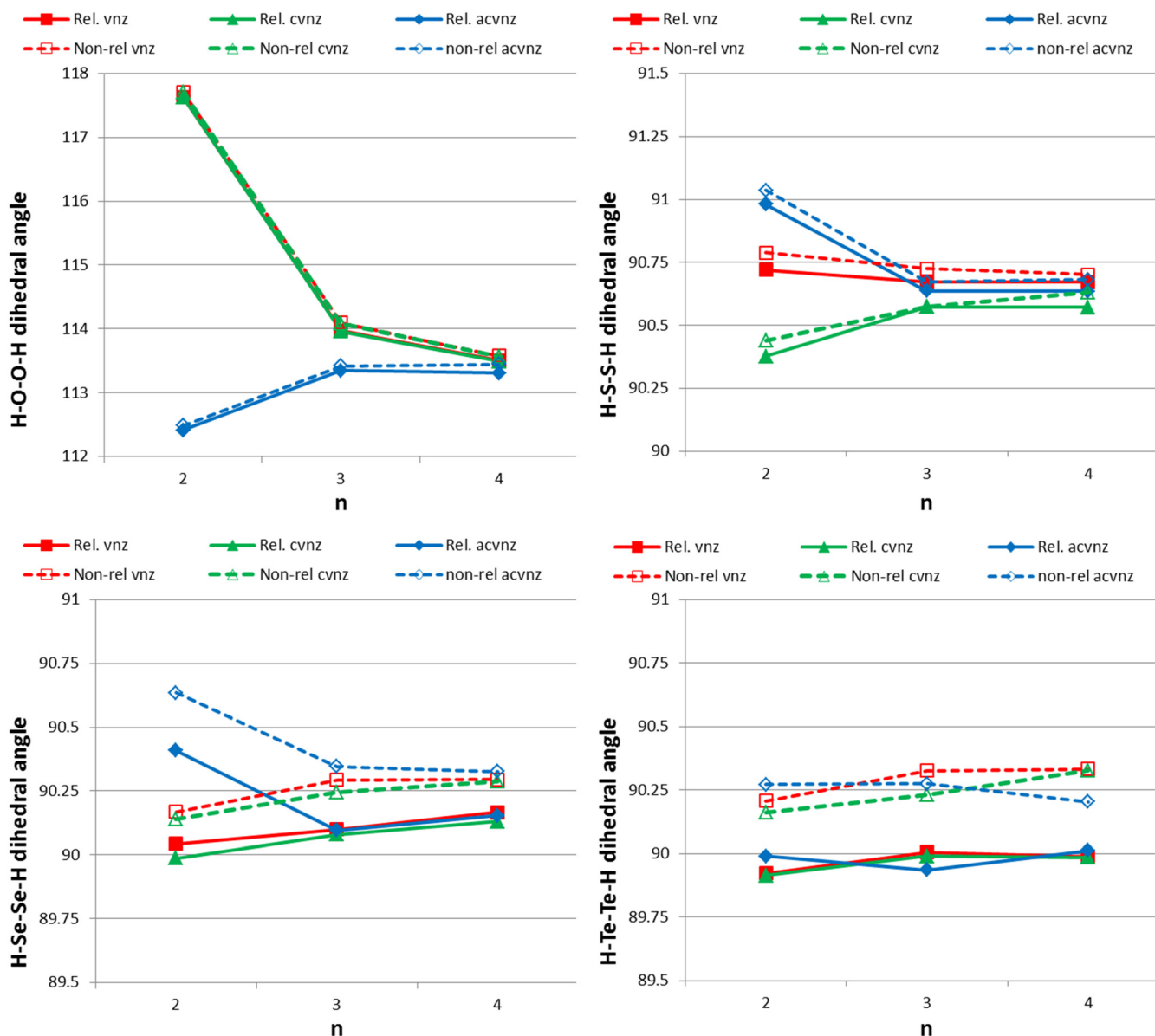


Figure 4. The H-X-X-H dihedral angle ($X = \text{O}, \text{S}, \text{Se}, \text{Te}$) versus cardinal numbers n of the dyall.vnz , dyall.cvnz , and dyall.acvnz obtained in four-component (“Rel” and solid lines) and nonrelativistic (“Non-rel” and dashed lines) geometry optimizations using the B3LYP functional. Note the four times larger scale of the y-axis for H_2O_2 . Tables with the values are presented in the Supporting Information. [Color figure can be viewed at wileyonlinelibrary.com]

contrast to the X-X bonds. But again the difference is large for H_2O_2 . For H_2Se_2 and H_2Te_2 our optimized X-H bond lengths are 1.4747 Å and 1.6701 Å, respectively, calculated with the dyall.acv4z basis set.

For the two sets of angles, the X-X-H angles in Figure 3 and the dihedral angles in Figure 4, we observe a somewhat different picture, although the dyall.vnz basis set results still differ for H_2S_2 and H_2Te_2 more from the results of the other basis sets than for the other two molecules. However, the diffuse functions in the acv2z basis set have a significantly larger impact on the angles than on the bond lengths. Sufficiently converged results for the X-X-H angles are again obtained already at the dyall.cv3z level with the exception of the dihedral angles in H_2O_2 and H_2S_2 , where again the diffuse functions have some influence. In general it is somewhat surprising to see that the

dihedral angle in H_2O_2 is much more basis set dependent than in the other molecules. The relativistic effects on the angles are percentagewise similar to the changes in the X-X bond lengths, 0.1% to 0.2%, and make both angles smaller.

Compared with the experimentally measured X-X-H angles,^[41,42] 94.8° in H_2O_2 and 97.88° in H_2S_2 our four-component dyall.acv4z calculated values 100.78° and 98.70° are in good agreement for H_2S_2 but exhibit a larger deviation, 6%, for H_2O_2 . The same holds also for the dihedral angles, where the measured values are 119.8° and 90.3° and the four-component dyall.acv4z calculated ones 113.31° and 90.64° for H_2O_2 and H_2S_2 , respectively. We, thus, note that in general the B3LYP optimized structure of H_2O_2 is in less good agreement with the experimental values than the geometry of H_2S_2 . The four-component dyall.acv4z optimized angles for the other two

Table 3. X-H one-bond reduced coupling constants (in $10^{19} \text{ J}^{-1} \text{ T}^2$) calculated at the four-component and nonrelativistic DFT/B3LYP level with various basis sets.

K^{XH}	dyall.acv2z		dyall.acv3z		dyall.acv4z	
	No-rel	Rel	No-rel	Rel	No-rel	Rel
$^1\text{H}_2^{17}\text{O}_2$	27.23	26.98	29.70	29.42	30.37	30.09
$^1\text{H}_2^{33}\text{S}_2$	12.19	10.65	11.96	10.29	12.19	10.48
$^1\text{H}_2^{77}\text{Se}_2$	-25.35	-45.49	-29.63	-52.16	-29.98	-52.85
$^1\text{H}_2^{125}\text{Te}_2$	-32.75	-108.82	-38.27	-120.88	-38.68	

compounds are: Se-Se-H angle 96.66° , Te-Te-H angle 95.88° , H-Se-Se-H angle 90.15° , and H-Te-Te-H angle 90.01° .

For the following calculations of the coupling constants and coupling constant polarizabilities the dyall.acv3z geometry has been employed.

Reduced one-bond spin-spin coupling constants

In Table 3, the results for the reduced one-bond X-H coupling constants are shown. They were calculated both at the four-component and nonrelativistic level with B3LYP functional with the dyall.acvnz basis sets. The influence of the basis set is significant on going from the double- ζ to the triple- ζ basis sets: $\sim 9\%$ for H_2O_2 and $\sim 17\%$ for both H_2Se_2 and H_2Te_2 at the nonrelativistic level and somewhat smaller at the relativistic level. The equivalent change for H_2S_2 is much smaller, negative and the values with the double- ζ basis set actually larger in the relativistic case. However, the differences to the quadruple- ζ basis set are with 1% to 2% much smaller both at the relativistic and nonrelativistic level. We have, therefore, also omitted the calculations with the dyall.acv4z basis set for H_2Te_2 in the following.

While the relativistic and nonrelativistic results for the one bond O-H coupling are not quite identical, the differences are still less than 1%. But the relativistic effects become gradually larger with increasing nuclear charge so that they amount to 14% for the S-H coupling, 76% for the Se-H coupling and the Te-H coupling is at the four-component relativistic level more than 3 times as large as the nonrelativistic value—a change of 216%. The need for a relativistic description is, thus, very obvious in the case of spin-spin coupling constants involving for Se and Te, while a nonrelativistic description seems to suffice for O and almost for S. In addition one should notice that the reduced coupling constants change sign in this series of similar molecules, or expressed differently the one-bond X-H coupling becomes smaller along the series H_2O_2 , H_2S_2 , H_2Se_2 , H_2Te_2 and between S and Se negative, which indicates a systematic change in the electronic structure of these molecules as also seen from the increasing bond lengths and decreasing angles along this series.

Calculation of the reduced spin-spin coupling polarizability tensor $K_\gamma^{I_a J_b}$

In the following we will discuss the results of the calculations of reduced coupling polarizability vector A_γ^{XH} both at the four-component relativistic and the nonrelativistic level. The definition of the x , y , z axis is shown in Figure 5. The y axis is chosen

to coincide with the direction of the X-H bond in all molecules, that is, along the bond between the atoms, which coupling is studied. The X-X bond is in the x - y plane, and the z axis is perpendicular to this plane.

The components A_x and A_y of the reduced coupling constant polarizability vector are in general one or two orders of magnitude greater than the A_z -component, that is, for H_2O_2 $A_z/A_x \approx 0.09$, for H_2S_2 $A_z/A_x \approx 0.006$, for H_2Se_2 $A_z/A_x \approx 0.02$, and for H_2Te_2 $A_z/A_x \approx 0.008$. This behavior can be understood qualitatively considering a reflection with respect to the x - y plane. The isotropic coupling polarizability vector is a polar vector, therefore, applying a reflection with respect to that plane its components are transformed as

$$A'_x = A_x \quad (15a)$$

$$A'_y = A_y \quad (15b)$$

$$A'_z = -A_z \quad (15c)$$

Additionally, both the studied X-H bond and the X-X bond are contained in the x - y reflection plane, while the second X-H bond, which changes its orientation on the considered reflection, is relatively far away from the atoms of the studied coupling constant. Therefore, the vectors A and A' must be very similar to each other. And if the eq. 15c is taken into account, it follows that $A_z/A_x \ll 1$ and $A_z/A_y \ll 1$. Applying the same reasoning, the behavior of $A_z/A_x \approx 0.1$ for H_2O_2 , while $A_z/A_x \approx 0.01$ for the other molecules can be also understood. The O-O distance is significantly shorter than the X-X distance of the other systems, consequently it is expected that the other O-H bond, that is, the one that is out of the x - y plane, has greater influence on the polarization vector of the studied one-bond coupling.

The basis set dependence of the components of the reduced coupling polarizability vector, A_γ^{XH} [$\gamma = x, y, z$; eq. 9] is represented in Figures 6 and 7, for the dyall.acvnz basis sets with $n = 2, 3, 4$ for H_2O_2 , H_2S_2 , and H_2Se_2 , and $n = 2, 3$ for H_2Te_2 .

The A_x^{XH} and A_y^{XH} components increase somewhat with the basis set size, in both the relativistic and nonrelativistic calculations for all four compounds studied here. Particularly, the A_x^{XH} component increases by $\sim 3\%$ to $\sim 4\%$ from dyall.acv2z to dyall.acv3z at the nonrelativistic level. The same comparison for relativistic calculations gives increments in the order of $\sim 3\%$ to $\sim 5\%$ on going from the dyall.acv2z to dyall.acv3z basis sets for the four compounds. The comparison between dyall.acv3z and dyall.acv4z shows increments of only $\sim 0.5\%$ in both the

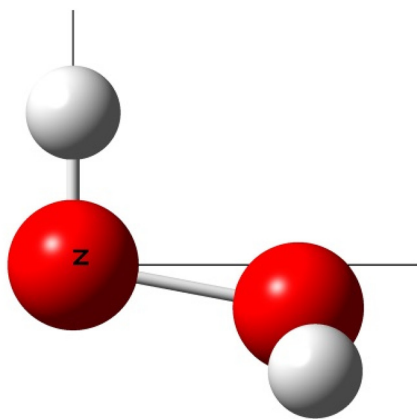


Figure 5. H_2X_2 geometry. The y axis has direction of $-\text{X}-\text{H}$ bond. The $\text{X}-\text{X}$ bond is in the x - y plane, and the z axis is perpendicular to this plane. [Color figure can be viewed at wileyonlinelibrary.com]

nonrelativistic and relativistic calculations, for compounds with O, S, and Se. The analysis of the A_y^{XH} component, which in itself is larger than the A_x^{XH} component, shows an increment of

$\sim 7.5\%$ on going from the dyall.acv2z to the dyall.acv3z basis set for H_2O_2 and H_2S_2 , and of $\sim 6\%$ and $\sim 4\%$ for H_2Se_2 and H_2Te_2 , respectively. The comparison between the dyall.acv3z and dyall.acv4z results shows increments of $\sim 1.9\%$ for H_2O_2 , $\sim 1.4\%$ for H_2S_2 , and $\sim 1.3\%$ for H_2Se_2 , respectively. Similar increments are observed for the corresponding relativistic calculations.

The A_z^{XH} components, Figure 7, are very small for all four molecules compared to the in-plane components A_x^{XH} and A_y^{XH} , ranging from $-0.3 \times 10^8 \text{ T}^2 \text{ m J}^{-1} \text{ V}^{-1}$ for H_2O_2 to $\sim 2 \times 10^8 \text{ T}^2 \text{ m J}^{-1} \text{ V}^{-1}$ for H_2Te_2 . It practically does not depend on the basis set size in the case of H_2O_2 . But for H_2S_2 , A_z^{XH} decreases by 33% on going from dyall.acv2z to dyall.acv3z and by $\sim 7\%$ from the dyall.acv3z to dyall.acv4z basis sets in the nonrelativistic calculations. For H_2Se_2 the same component decreases by $\sim 6\%$ on going from dyall.acv2z to dyall.acv3z and by $\sim 0.3\%$ from dyall.acv3z to dyall.acv4z also in the nonrelativistic calculation. In the relativistic calculations, the decrease is $\sim 18\%$ on going from dyall.acv2z to dyall.acv3z and $\sim 3\%$ from dyall.acv3z to dyall.acv4z for H_2S_2 . Conversely, for H_2Se_2 the result increases by $\sim 2.2\%$ on going from dyall.acv2z to dyall.

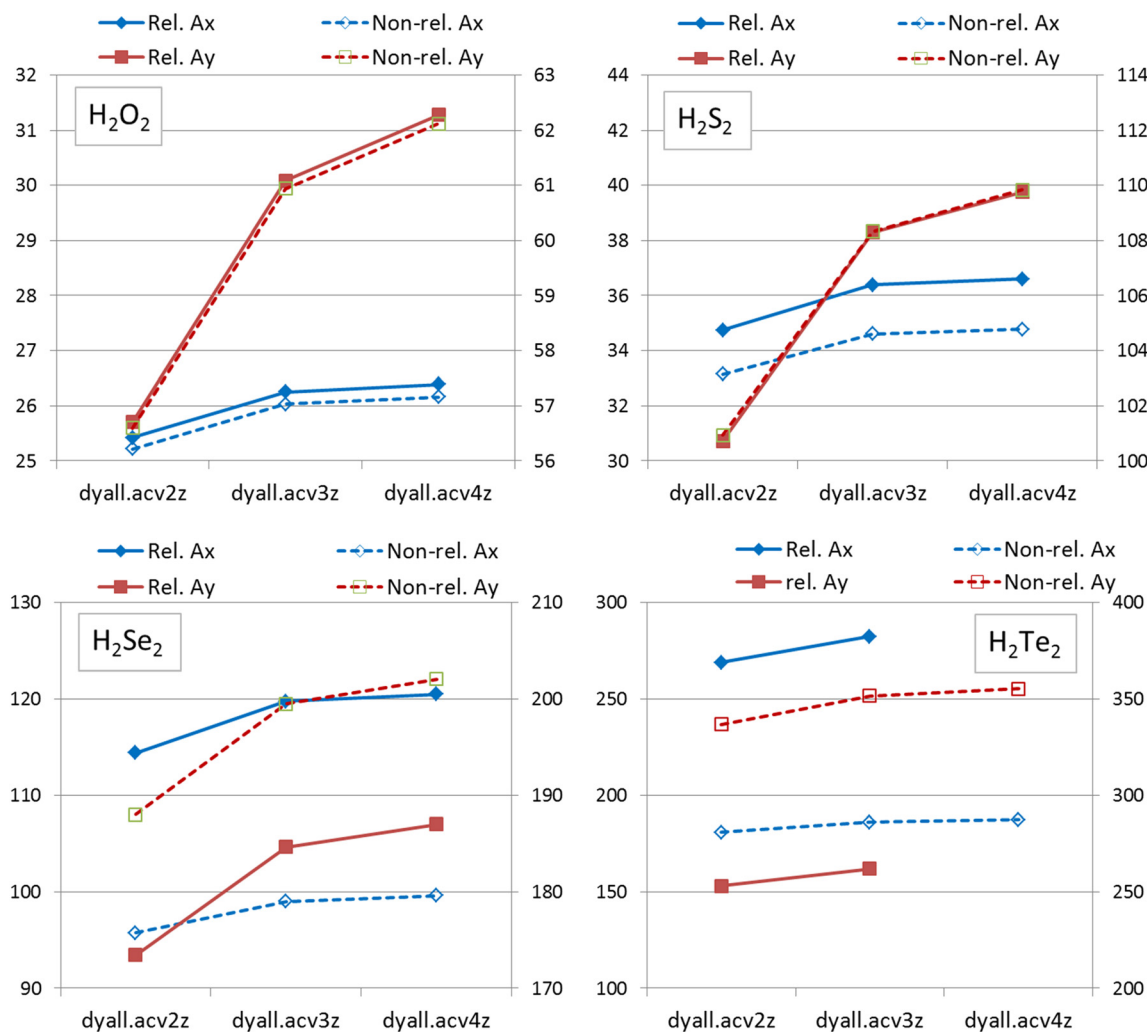


Figure 6. Basis set dependence of the x - and y -components of the reduced of spin-spin coupling constant polarizability vector \mathbf{A} ($10^8 \text{ T}^2 \text{ m J}^{-1} \text{ V}^{-1}$) at the DTF/B3LYP level with the dyall.acv n z basis sets ($n = 2, 3, 4$). The left axes are for the x -components and the right axes are for the y -components. [Color figure can be viewed at wileyonlinelibrary.com]

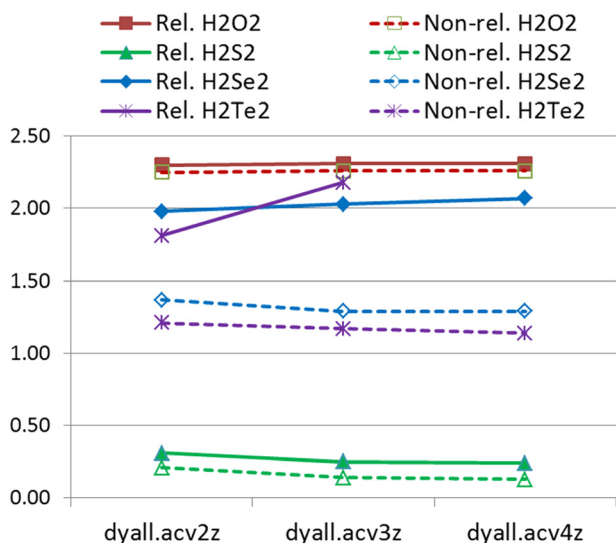


Figure 7. Basis set dependence of the z-components of the reduced of spin-spin coupling constant polarizability vector \mathbf{A} ($10^8 \text{ T}^2 \text{ m J}^{-1} \text{ V}^{-1}$) at the DTF/B3LYP level with the dyall.acv n z basis sets ($n = 2, 3, 4$). [Color figure can be viewed at wileyonlinelibrary.com]

acv3z and by $\sim 2.1\%$ from dyall.acv3z to dyall.acv4z. From this analysis, it becomes clear that the calculations are sufficiently converged with the dyall.acv3z basis set, differing in less than 2.5% from dyall.acv4z basis set results. The only exception is the A_z^{SH} component for H₂S₂ in the nonrelativistic calculation. However, the z-component is so much smaller than the other two components.

For the H₂Te₂ molecule, due to limited computational resources, we did not carry out the relativistic calculation with the dyall.acv4z basis set. The convergence of the results reported for H₂O₂, H₂S₂, and H₂Se₂ in Table 3 and Figures 6–8 suggests, however, that the dyall.acv3z basis set should be close to convergence also for H₂Te₂ and in particular is sufficient for estimating the importance of relativistic effects on the coupling constant polarizability. We also evaluated the reduced coupling polarizability vector at the no-relativistic level employing the dyall.acv4z basis for H₂Te₂, the A_x^{TeH} and A_y^{TeH} components increase by $\sim 1\%$ from dyall.acv3z to dyall.acv4z, while the much smaller A_z^{TeH} component decreases by 2.6% from dyall.acv3z to dyall.acv4z.

Turning now to the importance of relativistic effects on the coupling constant polarizabilities, we observe that four-component relativistic results for the same components of the electric field derivatives of the isotropic reduced coupling are comparable to the nonrelativistic results in the case of H₂O₂ and H₂S₂, but differ significantly for H₂Se₂ and H₂Te₂. Including relativistic effects always increase the smaller A_x - and A_z -components, while it reduces the larger A_y -component. For H₂S₂ the A_x^{SH} -component is, thus, increased by 5%, while the other two components like all the components for H₂O₂ are only marginally changed. In H₂Se₂ the A_x^{SeH} -component is then already increased by 21% and the A_y^{SeH} -component is reduced by 7% in the relativistic calculation. In H₂Te₂, finally, relativistic effects increase the A_x^{TeH} -component by 52% and reduce the

A_y^{TeH} -component by 25%. These large changes lead to that the A_x^{TeH} -component, which is predicted to be smaller than the A_y^{TeH} -component by the nonrelativistic calculations, turns out to be larger in the relativistic calculations, as can be seen in Figure 6. Compared to the changes in the coupling constants in Table 3, we find a similar increase of the importance of relativistic corrections for the components of the coupling constant polarizability vector, but the relative changes in the coupling polarizability are nevertheless smaller.

The pseudoscalar $\overline{K}_{XH}^{(1)}$ of the reduced coupling constant polarizability tensor is for the four systems shown in Figure 8 calculated both at the four-component relativistic and nonrelativistic level using the dyall.acv3z basis set and the B3LYP functional. The corresponding values for the other basis sets are reported in the Supporting Information. There are two important observations to be made from Figure 8. First of all there is a systematic trend for $\overline{K}_{XH}^{(1)}$ in this series of molecules, where it changes from being negative for H₂O₂ to positive but small in H₂S₂ and then keeps on increasing to H₂Te₂. Second, Figure 8 allows us to appreciate the great importance of using relativistic calculations for the pseudoscalar $\overline{K}_{XH}^{(1)}$ in the molecules containing Se and Te, H₂Se₂ and H₂Te₂. The relativistic values are ~ 5 times larger for the Se and 20 times larger for the Te-compound, while for S it is a factor 3.5 and none for O. The relative relativistic effects on the pseudoscalar are, thus, much larger than for the components of the coupling constant polarizability vector A_y^{XH} or the reduced coupling constants.

One should remember that it is this pseudoscalar $\overline{K}_{XH}^{(1)}$, which is important for the discrimination of chiral molecules by NMR. The trend of an increasing pseudoscalar in this series of molecules, in particular after considering relativistic effects, hints that the suggested chiral discrimination might be possible in compounds containing Se and Te. This possibility has recently already been supported by calculations on cyclic systems containing Se and Te reporting pseudoscalars of the related nuclear magnetic shieldings polarizabilities which were two orders of magnitude larger than those previously reported.^[12]

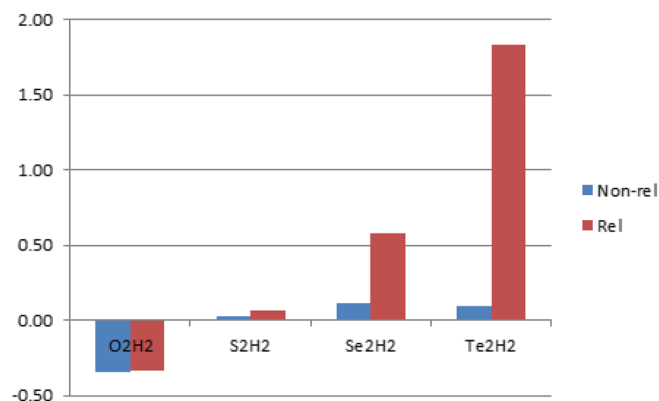


Figure 8. The pseudoscalar, $\overline{K}_{XH}^{(1)}$ (in $10^8 \text{ T}^2 \text{ m J}^{-1} \text{ V}^{-1}$), associated with the reduce spin-spin coupling polarizability tensor calculated at the DTF/B3LYP level with the basis set dyall.acv3z. [Color figure can be viewed at wileyonlinelibrary.com]

Finally, we consider important some discussion about further comparison with experimental results, when they will be available. Vibrational corrections, not considered here, are many times important for getting good agreement with experimental values.^[45] Previous articles on the kind of coupling constants encountered in this work^[38,46] show that those corrections could be between 0.1% to 3%. To fulfill the reproduction of the typical experimental setup one should also include solvent effects, which nowadays can be treated either by continuum solvation models^[47] or combined quantum and classical (QM/MM) methods,^[48] and which we neither included yet in our calculations.

Conclusions

We have investigated by four-component relativistic calculations at the DFT/B3LYP level whether it would become possible to use NMR spectroscopy and in particular the changes in the indirect nuclear spin–spin coupling constants to achieve chiral discrimination for molecules with larger nuclear charge and, thus, larger relativistic effects. For this purpose, we have investigated the pseudoscalar of the spin–spin coupling constants polarizability tensor for a series of chiral model compounds: H₂O₂, H₂S₂, H₂Se₂, and H₂Te₂.

In a first step, we have optimized the geometries of all four molecules both at the four-component relativistic and at the nonrelativistic level with Dyall's relativistic basis sets. We find that the extra diffuse functions in the augmented basis sets are of no importance for the optimization of the geometry with maybe the exception of the bond angles in the smallest basis sets. Overall, the dyall.cv3z basis set turned out to lead to geometry close to convergence for all four molecules both at the relativistic and nonrelativistic level. Interestingly, the dyall.vnz basis set was for S found to give results more differing from the results obtained with the larger basis sets than for the other atoms, possibly indicating a deficiency in this basis set for the third row atoms. With respect to relativistic effects on the geometry, we observe that the X–X bonds become longer, while the X–H bonds are shortened and the bond and dihedral angles are reduced.

For the reduced one-bond X–H coupling constant and its reduced coupling constant polarizability vector and pseudoscalar we find that the results are also close to convergence with the dyall.acv3z basis set.

The reduced coupling constants change systematically in the series of molecules from being positive for H₂O₂ and H₂S₂ to negative for H₂Se₂ and H₂Te₂. Also the relativistic effects increase along this series and become important for the Se and in particular for the Te compound, where the relativistic value for the coupling constant is about 3 times larger than the nonrelativistic value. This clearly shows again that relativistic effects cannot be ignored in calculations of NMR parameters for compounds with atoms like Se and Te.

For the reduced coupling constant polarizability vector A_{γ}^{XH} and for the isotropic pseudoscalar $\bar{K}_{XH}^{(1)}$ we observe that they significantly increase along the series of these molecules. This increase becomes even more important on inclusion of

relativistic effects. Their importance for the pseudoscalar $\bar{K}_{XH}^{(1)}$ in the molecules with Se and Te is remarkable. $\bar{K}_{XH}^{(1)}$ becomes 5 times as large for H₂Se₂ and 20 times as large for H₂Te₂ from a nonrelativistic to the relativistic calculation.


The ability to discriminate enantiomers in NMR spectroscopy is linked to the value of this pseudoscalar. Supported by the increasing coupling constant polarizabilities with heavier nuclei, our calculations suggest that enantiomeric discrimination is experimentally possible in molecules containing heavy nuclei.

Funding

This work was developed with financial support from Universidad de Buenos Aires (UBACYT 20020130100039BA), CONICET (PIP 11220130100377)

Keywords: Chiral discrimination · Nuclear magnetic resonance spectroscopy · spin-spin coupling constant · Electric dipole polarizability of nuclear spin-spin coupling · Relativistic effects

How to cite this article: G. I. Pagola, M. A. B. Larsen, M. Ferraro, S. P. A. Sauer. *J. Comput. Chem.* **2018**, *39*, 2589–2600. DOI: 10.1002/jcc.25648

 Additional Supporting Information may be found in the online version of this article.

- [1] D. Parker, *Chem. Rev.* **1991**, *91*, 1441.
- [2] I. Canet, J. Courtieu, A. Loewenstein, A. Meddour, J. M. Pechine, *J. Am. Chem. Soc.* **1995**, *117*, 6520.
- [3] M. Raban, K. Mislow, *Tetrahedron Lett.* **1965**, *6*, 4249.
- [4] G. M. Whitesides, D. W. Lewis, *J. Am. Chem. Soc.* **1970**, *92*, 6979.
- [5] A. Buckingham, *Chem. Phys. Lett.* **2004**, *398*, 1.
- [6] A. Buckingham, P. Fischer, *Chem. Phys.* **2006**, *324*, 111.
- [7] S. Pelloni, P. Lazzeretti, R. Zanasi, *J. Chem. Theory Comput.* **2007**, *3*, 1691.
- [8] R. Zanasi, S. Pelloni, P. Lazzeretti, *J. Comput. Chem.* **2007**, *28*, 2159.
- [9] G. I. Pagola, M. B. Ferraro, S. Pelloni, P. Lazzeretti, S. P. A. Sauer, *Theor. Chem. Acc.* **2011**, *129*, 359.
- [10] H. Kjær, S. P. A. Sauer, J. Kongsted, *J. Comput. Chem.* **2011**, *32*, 3168.
- [11] H. Kjær, M. R. Nielsen, G. I. Pagola, M. B. Ferraro, P. Lazzeretti, S. P. A. Sauer, *J. Comput. Chem.* **2012**, *33*, 1845.
- [12] S. Pelloni, F. Faglioni, P. Lazzeretti, *Rend. Fis. Acc. Lincei* **2013**, *24*, 283.
- [13] (a) S. Komorovsky, M. Repisky, K. Ruud, O. L. Malkina, V. G. Malkin, *J. Phys. Chem. A* **2013**, *117*, 14209. (b) Y. Y. Rusakov, I. L. Rusakova, L. B. Krivdin, *Magn. Reson. Chem.* **2014**, *52*, 214. (c) I. L. Rusakova, Y. Y. Rusakov, L. B. Krivdin, *Magn. Reson. Chem.* **2014**, *52*, 500. (d) A. Křístková, S. Komorovsky, M. Repisky, V. G. Malkin, O. L. Malkina, *J. Chem. Phys.* **2015**, *142*, 114102. (e) Y. Y. Rusakov, L. B. Krivdin, *J. Comput. Chem.* **2015**, *36*, 1756. (f) I. L. Rusakova, Y. Y. Rusakov, L. B. Krivdin, *J. Comput. Chem.* **2016**, *37*, 1367. (g) M. Jankowska, T. Kupka, L. Stobiński, R. Faber, E. G. Lacerda, Jr., S. P. A. Sauer, *J. Comput. Chem.* **2016**, *37*, 395. (h) I. L. Rusakova, Y. Y. Rusakov, L. B. Krivdin, *J. Phys. Chem. A* **2017**, *121*, 4793. (i) I. L. Rusakova, Y. Y. Rusakov, L. B. Krivdin, *Russ. Chem. Rev.* **2016**, *85*, 356. (j) I. L. Rusakova, L. B. Krivdin, *Mendeleev Commun.* **2018**, *28*, 1. (k) E. G. Lacerda, Jr., S. P. A. Sauer, K. V. Mikkelsen, K. Coutinho, S. Canuto, *J. Mol. Model.* **2018**, *24*, 62.
- [14] I. Mills, T. Cvitas, K. Homann, N. Kallay, K. Kuchitsu, *Quantities, Units and Symbols in Physical Chemistry*; Blackwell Scientific Publications: Oxford, **1993**.
- [15] N. F. Ramsey, *Phys. Rev.* **1953**, *91*, 303.
- [16] S. P. A. Sauer, *Molecular Electromagnetism*, Oxford University Press: Oxford, **2011**.

- [17] G. I. Pagola, M. C. Caputo, M. B. Ferraro, P. Lazzarotti, *Phys. Rev. A* **2006**, 74, 022509.
- [18] (a) S. P. A. Sauer, *J. Chem. Phys.* **1993**, 98, 9220. (b) P. Lazzarotti, *J. Chem. Phys.* **2012**, 137, 74108.
- [19] T. Helgaker, M. Jaszczuński, K. Ruud, *Chem. Rev.* **1999**, 99, 293.
- [20] (a) G. A. Aucar, J. Oddershede, *Int. J. Quantum Chem.* **1993**, 47, 425. (b) G. A. Aucar, T. Saue, L. Visscher, H. J. A. Jensen, *J. Chem. Phys.* **1999**, 110, 6208.
- [21] T. Saue, H. J. A. Jensen, *J. Chem. Phys.* **2003**, 118, 522.
- [22] L. Visscher, T. Enevoldsen, T. Saue, H. J. A. Jensen, J. Oddershede, *J. Comput. Chem.* **1999**, 20, 1262.
- [23] P. Norman, H. J. A. Jensen, *J. Chem. Phys.* **2004**, 121, 6154.
- [24] J. Henriksson, T. Saue, P. Norman, *J. Chem. Phys.* **2008**, 128, 024105.
- [25] J. Olsen, P. Jørgensen, *J. Chem. Phys.* **1985**, 82, 3235.
- [26] O. Christiansen, P. Jørgensen, C. Hättig, *Int. J. Quantum Chem.* **1998**, 68, 1.
- [27] H. Hettema, H. J. Aa, P. J. Jensen, J. Olsen, *J. Chem. Phys.* **1992**, 97, 1174.
- [28] O. Vahtras, H. Ågren, P. Jørgensen, H. J. A. Jensen, S. B. Padkjær, T. Helgaker, *J. Chem. Phys.* **1992**, 96, 6120.
- [29] T. Helgaker, M. Watson, N. C. Handy, *J. Chem. Phys.* **2000**, 113, 9402.
- [30] T. Saue, K. Fægri, Jr., T. Helgaker, O. Gropen, *Mol. Phys.* **1997**, 91, 937.
- [31] K. G. Dyall, K. Fægri, Jr., *Introduction to Relativistic Quantum Chemistry*, Oxford University Press: Oxford, **2007**.
- [32] T. Saue, H. J. A. Jensen, *J. Chem. Phys.* **1999**, 111, 6211.
- [33] (a) H. J. Aa. Jensen, R. Bast, T. Saue, and L. Visscher, with contributions from V. Bakken, K. G. Dyall, S. Dubillard, U. Ekström, E. Eliav, T. Enevoldsen, T. Fleig, O. Fossgaard, A. S. P. Gomes, T. Helgaker, J. K. Lærdahl, Y. S. Lee, J. Henriksson, M. Ilias, Ch. R. Jacob, S. Knecht, S. Komarovsk'y, O. Kullie, C. V. Larsen, H. S. Nataraj, P. Norman, G. Olejniczak, J. Olsen, Y. C. Park, J. K. Pedersen, M. Pernpointner, K. Ruud, P. Salek, B. Schimmelpfennig, J. Sikkema, A. J. Thorvaldsen, J. Thyssen, J. van Stralen, S. Villaume, O. Visser, T. Winther, and S. Yamamoto DIRAC, A Relativistic Ab Initio Electronic Structure Program, Release DIRAC14.0, 2014. Available at: <http://www.diracprogram.org>; (b) Bast, T. Saue, L. Visscher, and H. J. Aa. Jensen, with contributions from V. Bakken, K. G. Dyall, S. Dubillard, U. Ekstroem, E. Eliav, T. Enevoldsen, E. Fasshauer, T. Fleig, O. Fossgaard, A. S. P. Gomes, T. Helgaker, J. Henriksson, M. Ilias, Ch. R. Jacob, S. Knecht, S. Komarovskiy, O. Kullie, J. K. Laerdahl, C. V. Larsen, Y. S. Lee, H. S. Nataraj, M. K. Nayak, P. Norman, G. Olejniczak, J. Olsen, Y. C. Park, J. K. Pedersen, M. Pernpointner, R. Di Remigio, K. Ruud, P. Salek, B. Schimmelpfennig, J. Sikkema, A. J. Thorvaldsen, J. Thyssen, J. van Stralen, S. Villaume, O. Visser, T. Winther, and S. Yamamoto, DIRAC, a relativistic ab initio electronic structure Dent. Prog., Release DIRAC15, 2015. Available at: <http://www.diracprogram.org>
- [34] K. Aidas, C. Angeli, K. L. Bak, V. Bakken, R. Bast, L. Boman, O. Christiansen, R. Cimraglia, S. Coriani, P. Dahle, E. K. Dalskov, U. Ekström, T. Enevoldsen, J. J. Eriksen, P. Ettenhuber, B. Fernández, L. Ferrighi, H. Fliegl, L. Frediani, K. Hald, A. Halkier, C. Hättig, H. Heiberg, T. Helgaker, A. C. Hennum, H. Hettema, E. Hjertenæs, S. Høst, I.-M. Høyvik, M. F. Iozzi, B. Jansik, H. J. A. Jensen, D. Jonsson, P. Jørgensen, J. Kauczor, S. Kirpekar, T. Kjærgaard, W. Klopper, S. Knecht, R. Kobayashi, H. Koch, J. Kongsted, A. Krapp, K. Kristensen, A. Ligabue, O. B. Lutnæs, J. I. Melo, K. V. Mikkelsen, R. H. Myhre, C. Neiss, C. B. Nielsen, P. Norman, J. Olsen, J. M. H. Olsen, A. Osted, M. J. Packer, F. Pawłowski, T. B. Pedersen, P. F. Provasi, S. Reine, Z. Rinkevicius, T. A. Ruden, K. Ruud, V. V. Rybkin, P. Saek, C. C. M. Samson, A. S. de Meras, T. Saue, S. P. A. Sauer, B. Schimmelpfennig, K. Snedkov, A. H. Steindal, K. O. Sylvester-Hvid, P. R. Taylor, A. M. Teale, E. I. Tellgren, D. P. Tew, A. J. Thorvaldsen, L. Thøgersen, O. Vahtras, M. A. Watson, D. J. D. Wilson, M. Ziolkowski, H. Ågren, *WIREs Comput. Mol. Sci.* **2014**, 4, 269.
- [35] (a) K. G. Dyall, *Theor. Chem. Acc.* **1998**, 99, 366. (b) K. G. Dyall, *Theor. Chem. Acc.* **2002**, 108, 335. (c) K. G. Dyall, *Theor. Chem. Acc.* **2002**, 108, 365. (d) K. G. Dyall, *Theor. Chem. Acc.* **2004**, 112, 403. (e) K. G. Dyall, *Theor. Chem. Acc.* **2006**, 115, 441. (f) K. G. Dyall, *Theor. Chem. Acc.* **2007**, 117, 483. (g) K. G. Dyall, *Theor. Chem. Acc.* **2007**, 117, 491. (h) K. G. Dyall, *J. Phys. Chem. A* **2009**, 113, 12638. (i) K. G. Dyall, A. S. P. Gomes, *Theor. Chem. Acc.* **2009**, 125, 97. (j) K. G. Dyall, *Theor. Chem. Acc.* **2011**, 129, 603. (k) K. G. Dyall, *Theor. Chem. Acc.* **2012**, 131, 1172. (l) K. G. Dyall, *Theor. Chem. Acc.* **2012**, 131, 1217. (m) K. G. Dyall, *Theor. Chem. Acc.* **2016**, 135, 128.
- [36] (a) P. F. Provasi, G. A. Aucar, S. P. A. Sauer, *J. Chem. Phys.* **2001**, 115, 1324. (b) V. Barone, P. F. Provasi, J. E. Peralta, J. P. Snyder, S. P. A. Sauer, R. H. Contreras, *J. Phys. Chem. A* **2003**, 107, 4748. (c) P. F. Provasi and S. P. A. Sauer, *J. Chem. Phys.* **2010**, 133, 054308; (d) Y. Y. Rusakov, L. B. Krivdin, S. P. A. Sauer, E. P. Levanova, G. G. Levkovskaya, *Magn. Res. Chem.* **2010**, 48, 44. (e) E. D. Hedegård, J. Kongsted, S. P. A. Sauer, *J. Chem. Theory Comput.* **2011**, 7, 4077.
- [37] (a) F. Jensen, *J. Chem. Theory Comput.* **2006**, 2, 1360. (b) F. Jensen, *Theor. Chem. Acc.* **2010**, 126, 371. (c) P. A. Aggelund, S. P. A. Sauer, F. Jensen, *J. Chem. Phys.* **2018**, 149, 044117.
- [38] Y. Y. Rusakov, L. B. Krivdin, F. F. Østerstrøm, S. P. A. Sauer, V. A. Potapov, S. V. Amosova, *Phys. Chem. Chem. Phys.* **2013**, 15, 13101.
- [39] A. O. Dohn, K. B. Møller, S. P. A. Sauer, *Curr. Inorg. Chem.* **2013**, 3, 213.
- [40] S. P. A. Sauer, W. T. Raynes, *J. Chem. Phys.* **2000**, 113, 3121.
- [41] V. Burke, I. Grant, *Proc. Phys. Soc.* **1967**, 90, 297.
- [42] (a) T. Ziegler, J. G. Snijders, E. J. Baerends, *Chem. Phys. Lett.* **1980**, 75, 1. (b) J. G. Snijders, P. Pyykkö, *Chem. Phys. Lett.* **1980**, 75, 5.
- [43] R. L. Redington, W. B. Olson, P. C. Cross, *J. Chem. Phys.* **1962**, 36, 1311.
- [44] J. Behrend, P. Mittler, G. Winnewisser, K. Yamada, *J. Mol. Spectrosc.* **1991**, 150, 99.
- [45] (a) R. Faber, J. Kaminsky, S. P. A. Sauer, In *Gas Phase NMR*, Royal Society of Chemistry: Cambridge; K. Jackowski and M. Jaszczuński, Eds.; **2016**; Ch. 7, pp. 218–266; (b) R. D. Wigglesworth, W. T. Raynes, S. Kirpekar, J. Oddershede, S. P. A. Sauer, *J. Chem. Phys.* **2000**, 112, 736. (c) R. D. Wigglesworth, W. T. Raynes, S. Kirpekar, J. Oddershede, S. P. A. Sauer, *J. Chem. Phys.* **2001**, 114, 9192. (d) R. Faber, S. P. A. Sauer, *Phys. Chem. Chem. Phys.* **2012**, 14, 16440. (e) R. Faber, S. P. A. Sauer, *AIP Conf. Proc.* **2015**, 1702, 090035.
- [46] (a) R. D. Wigglesworth, W. T. Raynes, S. P. A. Sauer, J. Oddershede, *Mol. Phys.* **1997**, 92, 77.
- [47] (a) K. Ruud, L. Frediani, R. Cammi, B. Mennucci, *Int. J. Mol. Sci.* **2013**, 4, 119. (b) M. Pecul, K. Ruud, *Magn. Reson. Chem.* **2004**, 42, S128.
- [48] A. Møgelhøj, K. Aidas, K. V. Mikkelsen, S. P. A. Sauer, J. Kongsted, *J. Chem. Phys.* **2009**, 130, 134508.

Received: 29 July 2018

Revised: 18 September 2018

Accepted: 19 September 2018

Published online on 23 November 2018